

A Note on Plus-Contacts, Rectangular Duals, and Box-Orthogonal Drawings*

Therese Biedl[§] and Debajyoti Mondal[†]

[§]Cheriton School of Computer Science, University of Waterloo, Canada

[†]Department of Computer Science, University of Saskatchewan, Canada
biedl@uwaterloo.ca, dmondal@cs.usask.ca

November 5, 2018

Abstract

A plus-contact representation of a planar graph G is called c -balanced if for every plus shape $\mathbf{+}_v$, the number of other plus shapes incident to each arm of $\mathbf{+}_v$ is at most $c\Delta + O(1)$, where Δ is the maximum degree of G . Although small values of c have been achieved for a few subclasses of planar graphs (e.g., 2- and 3-trees), it is unknown whether c -balanced representations with $c < 1$ exist for arbitrary planar graphs.

In this paper we compute $(1/2)$ -balanced plus-contact representations for all planar graphs that admit a rectangular dual. Our result implies that any graph with a rectangular dual has a 1-bend box-orthogonal drawings such that for each vertex v , the box representing v is a square of side length $\frac{\deg(v)}{2} + O(1)$.

1 Introduction

Contact representation of planar graphs have been examined using different geometric objects (e.g., lines, rectangles, triangles, or circles) since the early 1980s [9, 7, 13, 15, 20]. Besides the intrinsic theoretical interest, such contact layouts find application in applied fields such as cartography, VLSI floor-planning, and data visualization. A rich body of literature examines contact layouts using polygons [2, 1, 9], T -shapes [8], L -shapes [14], and straight line segments [7].

We examine contact representations using *plus shapes* (i.e., a pair of intersecting vertical and horizontal line segments). A *plus-contact representation* of an n -vertex planar graph G is a non-crossing arrangement Γ_+ of n plus shapes such that each vertex v of G is mapped to a distinct plus shape $\mathbf{+}_v$ in Γ_+ and two plus shapes in Γ_+ touch if and only if the corresponding vertices are adjacent in G . If no arm of $\mathbf{+}_v$ is incident to more than $c\Delta + O(1)$ other arms, then Γ_+ is called a *c-balanced* representation, e.g., see Fig. 1(a)–(b).

Balanced plus-contact representations are motivated by the application of computing 1-bend box-orthogonal drawings with boxes of small size and constant aspect ratio [17, 21], e.g., see Fig. 1(b)–(d). A *1-bend box-orthogonal drawing* (resp., *1-bend Kandinsky drawing (KD)*) is a planar drawing, where each vertex is represented as an axis-aligned box (resp., square) and each edge is represented as an orthogonal polyline (with at most one bend) between the corresponding boxes. Every c -balanced plus-contact representation can be transformed into a 1-bend box-orthogonal drawing with square-size boxes of side length $c\Delta + O(1)$ [10]. Besides, balanced representations have been useful to construct planar drawings with small number of distinct edge slopes [10, 12]. Well balanced representations are known only for 2-trees ($1/4 \leq c \leq 1/3$)

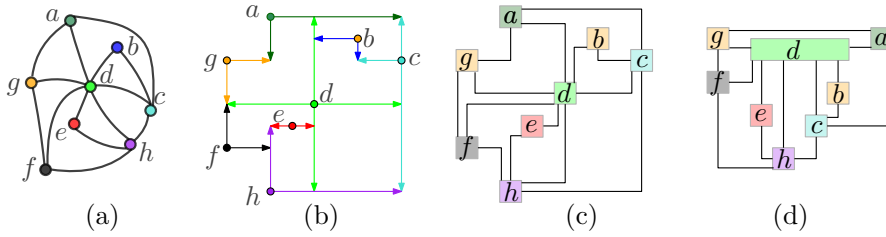


Figure 1: (a) A planar graph G . (b)–(c) A $(1/2)$ -balanced plus-contact representation of G , and a corresponding 1-bend box-orthogonal drawing. (d) Another box-orthogonal representation of G , where vertex d has a large side length.

and planar 3-trees ($1/3 \leq c \leq 1/2$) [10]. It is not yet known whether there exist c -balanced plus-contact representations for arbitrary planar graphs with $c < 1$.

We construct $(1/2)$ -balanced plus-contact representations of graphs that admit rectangular duals. These graphs are irreducible triangulations (see e.g. [11]), i.e., graphs where the outer-face has degree at least 4, all inner faces are triangles, and there are no triangles that are not face. Our result implies that these graphs have 1-bend box-orthogonal drawings with squares of side length at most $\frac{\deg(v)}{2} + O(1)$ for each vertex v . To our knowledge, this result is new. The closest related results are 2-bend planar drawings where the length of the longer side of the box of v is at most $\frac{\deg(v)}{2} + O(1)$ [4], or 1-bend planar drawing where the length of the longer side of the box of v is at most $\deg(v)$ [5]. If the planarity requirement is dropped, then there are 1-bend orthogonal drawings where the length of the longer side of the box is at most $\frac{\deg(v)}{2} + O(1)$ [5].

2 Preliminaries

Let R_1 and R_2 be two interior-disjoint rectangle in the plane. R_1 and R_2 are called *adjacent* if they intersect only at their boundaries, i.e., they touch but do not overlap. If R_1 and R_2 intersect at a single point then we call them *corner adjacent*, e.g., see c, d in Fig. 2(a). On the other hand, if R_1 and R_2 share a vertical (horizontal) line segment of non-zero length on their boundaries, then we call them *vertically (horizontally) adjacent*, e.g., see a, b in Fig. 2(a).

A *rectangular tiling* Γ is a partition of a rectangle into non-overlapping rectangles, e.g., see Fig. 2(a) and (c). This naturally defined a graph $g(\Gamma)$ by assigning one vertex per rectangle and adding edges if and only if the rectangles are adjacent. We allow four rectangles to meet at a point, which means that $g(\Gamma)$ may be nonplanar, e.g., see Fig. 6(a)–(b) in Appendix A. (Such graphs are also known as *map graphs*.) A graph G has a *rectangle contact representation* if there is a rectangular tiling Γ with $g(\Gamma) = G$. A *rectangular dual* R of a planar graph G is a rectangle contact representation with the additional constraint that no four rectangles in R meet at a point. Unlike rectangle contact representations, rectangular duals can exist only for planar graphs.

Two adjacent rectangles R_1 and R_2 in Γ are *comparable* if their shared segment coincides with a side of one of these rectangles (see a, b in Fig. 2(a)). Otherwise, we call them *incomparable* (see h, f in Fig. 2(c)). We use $R_1 \subseteq_y R_2$ (resp., $R_1 \subseteq_x R_2$) to denote that R_1 and R_2 are vertically (resp., horizontally) adjacent, and one side of R_1 is a subset of one side of R_2 , see Fig. 2(d). Γ is called *consistent* if every pair of adjacent rectangles in Γ is comparable, see Fig. 2(a). We create plus-contact representations initially only for consistent rectangle contact representations, and so need a result whose proof is in Appendix A.

Lemma 1 *For any rectangle contact representation \mathcal{R} there exists a consistent rectangle contact representation \mathcal{R}_c such that any comparable pair R_1, R_2 in \mathcal{R} has the same (vertical or horizontal) adjacency in \mathcal{R}_c along a segment of non-zero length. \mathcal{R}_c can be found in polynomial time.*

*Work of the authors is supported in part by NSERC.

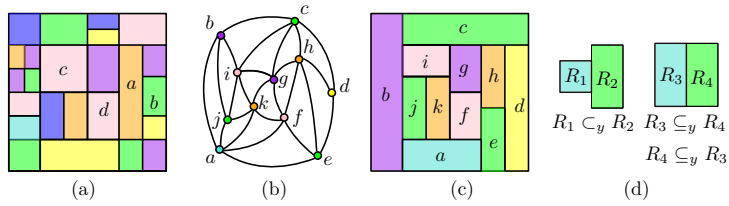


Figure 2: (a) A consistent rectangle contact representation. (b) A planar graph G . (c) A rectangular dual of G . (d) $R_1 \subset_y R_2$, $R_3 \subset_y R_4$.

Let G be a simple and connected planar graph. An *orthogonal drawing* Γ of G is a planar drawing of G in \mathbb{R}^2 , where each vertex of G is mapped to a point and each edge is mapped to an orthogonal polygonal chain between its corresponding end points. We call an orthogonal polygonal chain P a *zigzag path* if it is x or y -monotone, and contains at least two bend vertices. It is well-known that such zigzags can be eliminated in the following sense. Two orthogonal drawings Γ, Γ' of G are *equivalent* if for every vertex v with incident edge e , the attachment point of e at v (i.e., east, west, north, south) is the same in Γ and Γ' . Based on Tamassia's topology-shape-metric approach for orthogonal drawings, we have:

Lemma 2 ([19]) *For every planar orthogonal drawing, there exists an equivalent planar orthogonal drawing that does not contain any zigzag path.*

3 Drawing Algorithm

In this section we show that if G admits a rectangular dual \mathcal{R} , then it has a $(1/2)$ -balanced plus-contact representation Γ_+ . To compute Γ_+ , we first transform \mathcal{R} into a consistent rectangle contact representation \mathcal{R}_c using Lemma 1, and then transform \mathcal{R}_c into a $(1/2)$ -balanced plus-contact representation Γ of $g(\mathcal{R}_c)$. Finally, we will modify Γ to construct the required representation Γ_+ .

The representation Γ of the supergraph $g(\mathcal{R}_c)$ is already enough to construct a 1-bend box-orthogonal drawing of G with square-boxes of side length $\frac{\deg(v)}{2} + O(1)$ for every vertex v . Therefore, the transformation from Γ to Γ_+ (which involves a very large number of cases) is mostly of theoretical interest, and will be explained in detail only in Appendix B. For convenience, we will use the shortcut $\Delta_v := \frac{\deg(v)}{2} + O(1)$. Furthermore, we ignore floors and ceilings as they do not affect the asymptotic nature of our results.

From \mathcal{R}_c to Γ : Let v be a vertex represented by rectangle R in \mathcal{R}_c . We first add inside R two polygonal paths σ and σ' connecting the opposite corners of R ; see Fig. 3(a). These paths are such that after a 45° -rotation they would be xy -monotone orthogonal paths. At the intersection point c of σ and σ' the path from top-left to bottom-right uses \setminus while the other path uses $/$. Let the four *cords* of v be the four subpaths from c to the corners of c . The crucial insight is that the cords (after a 45° -rotation) become zig-zag paths, and so all bends can be removed by Lemma 2. Thus this shape is a plus-shape \dagger_v with c at the center and the four cords becoming the four arms.

We now extend the cords of the neighbours of v to realize the required adjacencies. These extensions may add more bends, but we will ensure that the extensions are xy -monotone paths (after a rotation) that begin and end with the same type of diagonal. Hence these are again zig-zag paths and all bends can be removed to obtain a plus-contact representation. We must ensure that at most Δ_v contacts are on each cord of v . Let R_1, \dots, R_t be the rectangles from left to right that are incident to the top boundary of R . We know that $R \subseteq_x R_1$ or $R_1 \subseteq_x R$ since we have a consistent rectangle contact representation. If $R \subseteq_x R_1$ then a contact representing this edge will be created inside R_1 , not inside R . So assume that $R_i \subseteq_x R$ for all $1 \leq i \leq t$. We choose the bottom-left cords of the first $t/2$ rectangles to touch the top-left cord of R , and the bottom-right cords of the remaining rectangles to touch the top-right cord of R using zigzag paths, as illustrated in Fig. 3(b). The treatment for the other sides is symmetric. The top-left

cord of R now has $\frac{\delta_t}{2} + \frac{\delta_l}{2} + O(1) \leq \mathbb{A}_v$ contacts, where δ_t and δ_l are the number of rectangles incident to the top and left sides of R , respectively. Similarly all other cords have at most \mathbb{A}_v contacts as desired.

Let the drawing determined by the cords of R be H , which we refer to as a *pseudo-plus representation*. Now rotate H by 45° to turn all cords into orthogonal xy -monotone paths. By Lemma 2, there exists an equivalent orthogonal drawing H' that contains no zigzag paths, which means that cords become straight-line segments, hence arms, and H' is the required plus-contact representation Γ .

Time Complexity: A rectangular dual \mathcal{R} of G can be computed in polynomial time (if it exists) [3, 16]. By Lemma 1, \mathcal{R} can be transformed into \mathcal{R}_c in polynomial time. Consider now the construction of the pseudo-plus representation H . The time complexity for this may initially appear high since cords may have many bends. However, instead of computing the pseudo-plus representation H explicitly, we only describe it implicitly via the topology-shape metric approach introduced by Tamassia [18]. This will lead to overall polynomial time.

Specifically, H can be described by defining a graph whose vertices are the ends of the cords, and whose edges are the parts of the cords between ends or contact points. At every center, the four incident face-angles are 90° . At every touching point we have one cord touching the interior of another, which gives two incident face-angles of 90° and one of 180° . At every end of a cord, we have some number of cords ending at the same point, but again, the incident face-angles are prescribed by our construction. Hence we know all face-angles at vertices. We also know that for any edge there exists a drawing such that the *bend-number* (defined to be the difference between left turns and right turns when walking from one end to the other) is 0. Since there exists an orthogonal drawing that respects these face-angles and bend-numbers, one can use the approach of Tamassia [18] to find an orthogonal drawing H' that realizes the face-angles and bend-numbers and has no zig-zags in polynomial time. This is the desired plus-contact representation.

From Γ to a 1-Bend Box-orthogonal drawing: Now convert Γ into a 1-bend box-orthogonal drawing as explained in [10]. Briefly, this places a box for v at the center of $\mathbf{+}_v$ and routes the edges along the arms of $\mathbf{+}_v$; with some offset to avoid overlap. Observe that G is a subgraph of $g(\mathcal{R}_c)$. Every four mutually adjacent rectangles $\{R_a, R_p, R_b, R_q\} \in \mathcal{R}_c$, give rise to exactly one adjacency in $g(\mathcal{R}_c)$ that is not in G , e.g., see Fig. 4(b). This undesired adjacency also appears in the plus-contact representation Γ and consequently in the 1-bend box-orthogonal drawing. However, we can simply remove this edge from the drawing, as illustrated in Fig. 4(c), and obtain:

Theorem 1 *Let G be a planar graph that admits a rectangular dual. Then G has a 1-bend box-orthogonal drawing, where each vertex v is a square of side length at most $\frac{\deg(v)}{2} + O(1)$.*

From Γ to Γ_+ : We would like to transform Γ to remove unnecessary adjacencies. Actually, we will modify the pseudo-plus representation H instead, since the changes require extending cords in different ways. The resulting pseudo-plus representation H^+ of G can be transformed into Γ_+ as before.

Consider Fig. 5(a). Let R_a, R_p, R_b, R_q be four mutually adjacent rectangles in \mathcal{R}_c , in this clockwise order around their common corner z and starting with the bottom-left rectangle. One

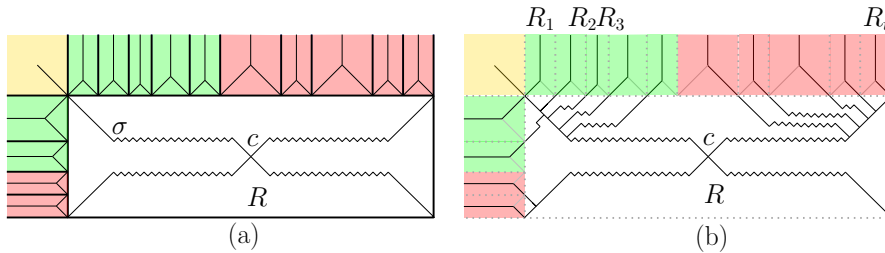


Figure 3: (a) Construction of the cords of R . (b) Extension of the cords of the rectangles that are adjacent to R . Only the rectangles that lie above or to the left of R are shown.

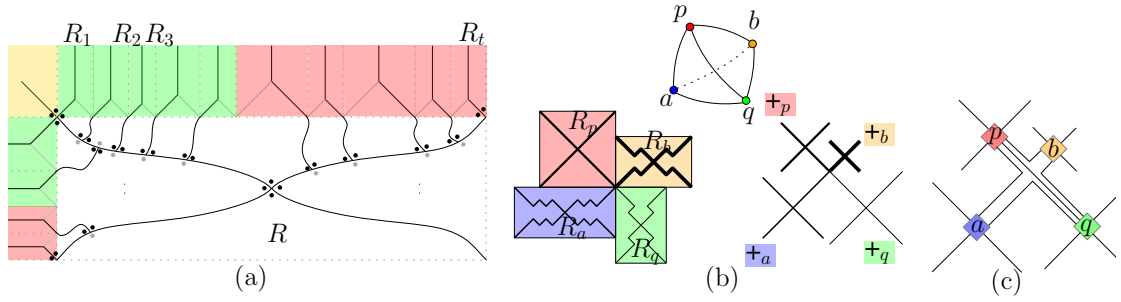


Figure 4: (a) Construction of the cords of R . The 90° and 180° angles are marked in black and gray dots, respectively. (b) Transformation into 1-bend Box orthogonal drawings.

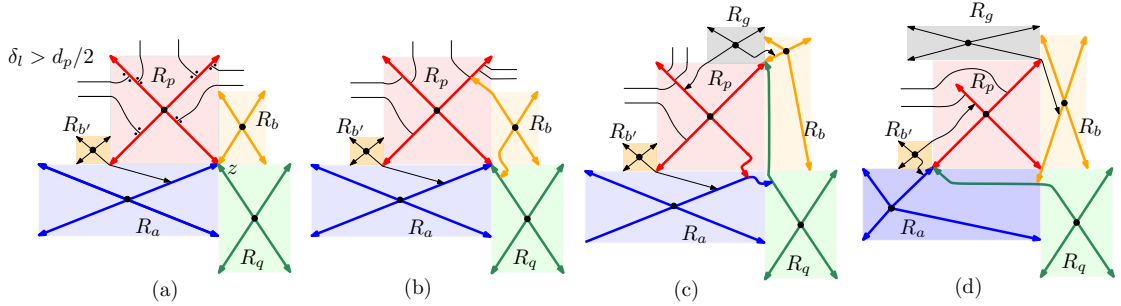


Figure 5: Illustration for Case 1a, where $\delta_l > d_p/2$. (a) Schematic representation of the initial configuration. The plus shapes are drawn with bidirected lines. The thin lines represent the distribution of $\delta_l, \delta_r, \delta_t, \delta_b$ to the four cords of R . The black dots represent 90° angles. (b-d) Resolution for various sub-cases.

of the edges (a, b) or (p, q) did not exist in G , say (a, b) was unnecessary. We refer to R_a, R_b as an *excess pair*, and R_p as the *consumer* of this excess pair. Put differently, the consumer of an unnecessary edge (a, b) is the upper one of the two rectangles that share a corner with R_a and R_b . We re-route locally near the consumer R_p such that (A) all unnecessary adjacencies for which R_p is the consumer have been removed, (B) all other adjacencies within the neighbours of R_p have been retained, (C) no new unnecessary adjacency is introduced, (D) all cords remain xy -monotone paths (after a 45° rotation), and (E) the cords of R_p remain $(1/2)$ -balanced.

The details of processing a consumer R_p are unfortunately quite tedious; Fig. 5 shows three of the (many) cases and Appendix B gives full details. Applying this to all consumers gives a pseudo-plus representation of G , which can be transformed to Γ_+ , and we obtain:

Theorem 2 *Let G be a planar graph that admits a rectangular dual. Then G has a plus-contact representation where for each vertex v each arm of \dagger_v has at most $\frac{\deg(v)}{2} + O(1)$ contacts with other plus-shapes.*

4 Conclusion

We have shown that every planar graph with a rectangular dual has a $(1/2)$ -balanced plus-contact representation and a 1-bend box-orthogonal drawing with square-size boxes of side length $\frac{\deg(v)}{2} + O(1)$ (for each vertex v). Both representations can be computed in polynomial time. While our results hold for all 4-connected planar graphs with four outer vertices, it remains open whether every planar graph admits a c -balanced representation for some $c < 1$.

References

- [1] M. J. Alam, T. Biedl, S. Felsner, A. Gerasch, M. Kaufmann, and S. G. Kobourov. Linear-time algorithms for hole-free rectilinear proportional contact graph representations. *Algorithmica*, 67(1):3–22, 2013.
- [2] M. J. Alam, D. Eppstein, M. T. Goodrich, S. G. Kobourov, and S. Pupyrev. Balanced circle packings for planar graphs. In *Proceedings of the 22nd International Symposium on Graph Drawing (GD)*, volume 8871 of *LNCS*, pages 125–136. Springer, 2014.
- [3] J. Bhasker and S. Sahni. A linear algorithm to find a rectangular dual of a planar triangulated graph. *Algorithmica*, 3:247–278, 1988.
- [4] T. Biedl and G. Kant. A better heuristic for orthogonal graph drawings. *Computational Geometry*, 9(3):159–180, 1998.
- [5] T. Biedl and M. Kaufmann. Area-efficient static and incremental graph drawings. In *Proceedings of the 5th Annual European Symposium on Algorithms (ESA)*, volume 1284 of *LNCS*, pages 37–52. Springer, 1997.
- [6] T. Biedl, A. Lubiw, M. Petrick, and M. J. Spriggs. Morphing orthogonal planar graph drawings. *ACM Transactions on Algorithms*, 9(4):29, 2013.
- [7] H. de Fraysseix, P. O. de Mendez, and J. Pach. Representation of planar graphs by segments. *Intuitive Geometry*, 63:109–117, 1991.
- [8] H. de Fraysseix, P. O. de Mendez, and P. Rosenstiehl. On triangle contact graphs. *Combinatorics, Probability and Computing*, 3(2):233–246, 1994.
- [9] C. A. Duncan, E. R. Gansner, Y. F. Hu, M. Kaufmann, and S. G. Kobourov. Optimal polygonal representation of planar graphs. *Algorithmica*, 63(3):672–691, 2012.
- [10] S. Durocher and D. Mondal. On balanced \vdash -contact representations. In *Proceedings of the 21st International Symposium on Graph Drawing (GD)*, volume 8242, pages 143–154. Springer, 2013.
- [11] É. Fusy. Transversal structures on triangulations: A combinatorial study and straight-line drawings. *Discrete Mathematics*, 309(7):1870–1894, 2009.
- [12] E. D. Giacomo, G. Liotta, and F. Montecchiani. 1-bend upward planar drawings of SP-digraphs. In Y. Hu and M. Nöllenburg, editors, *Proceedings of the 24th International Symposium on Graph Drawing and Network Visualization (GD)*, volume 9801 of *LNCS*, pages 123–130. Springer, 2016.
- [13] S. G. Kobourov, D. Mondal, and R. I. Nishat. Touching triangle representations for 3-connected planar graphs. In *Proceedings of the 20th International Symposium on Graph Drawing (GD)*, volume 7704, pages 199–210. Springer, 2012.
- [14] S. G. Kobourov, T. Ueckerdt, and K. Verbeek. Combinatorial and geometric properties of planar Laman graphs. In *Proceedings of the 24th Annual ACM-SIAM Symposium on Discrete Algorithms (SODA)*, pages 1668–1678. SIAM, 2013.
- [15] P. Koebe. Kontaktprobleme der konformen Abbildung. *Ber. Sächs. Akad. Wiss. Leipzig, Math.-Phys. Kl.*, 88:141–164, 1936.
- [16] K. Kozminski and E. Kinnen. Rectangular duals of planar graphs. *Networks*, 15(2):145–157, 1985.
- [17] A. Papakostas and I. G. Tollis. Efficient orthogonal drawings of high degree graphs. *Algorithmica*, 26(1):100–125, 2000.

- [18] R. Tamassia. On embedding a graph in the grid with the minimum number of bends. *SIAM Journal on Computing*, 16(3):421–444, 1987.
- [19] R. Tamassia and I. Tollis. Planar grid embedding in linear time. *IEEE Transactions on Circuits and Systems*, 36(9):1230–1234, 1989.
- [20] C. Thomassen. Interval representations of planar graphs. *J. Comb. Theory, Ser. B*, 40(1):9–20, 1986.
- [21] D. R. Wood. Multi-dimensional orthogonal graph drawing with small boxes. In *Proceedings of the 7th International Symposium on Graph Drawing (GD)*, volume 1731 of *LNCS*, pages 311–322. Springer, 1999.

Appendix A

Lemma 1 *For any rectangle contact representation \mathcal{R} there exists a consistent rectangle contact representation \mathcal{R}_c such that any comparable pair R_1, R_2 in \mathcal{R} has the same (vertical or horizontal) adjacency in \mathcal{R}_c along a segment of non-zero length. \mathcal{R}_c can be found in polynomial time.*

Proof: The idea is to process the incomparable pairs of \mathcal{R} one after another, and at each step ensuring that no adjacency in \mathcal{R} is destroyed. Every rectangle contact representation can be transformed into an equivalent grid representation, i.e., when the endpoints of all the line segments have integral coordinates. Therefore, we may assume that \mathcal{R} is a grid representation.

Here we describe how to remove an incomparable pair that is vertically adjacent. The treatment for the horizontally adjacent incomparable pairs is symmetric. Let R_p and R_q be a pair of vertically adjacent rectangles, which are incomparable. Let ab be the common vertical segment on the boundary of R_p and R_q . Without loss of generality assume that R_p lies to the left of R_q , and a and b are the top-left and bottom-right corners of R_q and R_p , respectively. Fig. 7 illustrates such a scenario.

We now modify \mathcal{R} such that the segment ab becomes degenerate, and R_p and R_q become corner adjacent. We first define a cut that partitions \mathcal{R} into two smaller drawings, as follows. Let s and t be two points with coordinates $(x(b)+\alpha, y(b)-\alpha)$ and $(x(a)+\alpha, y(a)+\alpha)$, respectively, for some constant α , where $0 < \alpha < 1$. Then the cut is an orthogonal polygonal chain $L = (s', s, t, t')$, where s' and t' lie on the left and right boundary of \mathcal{R} , respectively. See Fig. 7(a). The notion of cut has previously been used in the literature in more generalized settings, e.g., in the context of morphing orthogonal drawings [6].

Let Γ_t be the drawing that consists of all the points of Γ lying above L . We move all the points of Γ_t upward by $|ab|$ units, except the points that lie on the boundary of R_q . Consequently, the segment ab becomes degenerate. Let R_t be the rectangle that contains the point t . Observe that if L intersects the left boundary of a rectangle in $R \notin \{R_t, R_q\}$, then it also intersects its right boundary at the same height. Hence each of these rectangles can be recovered by extending the left and right boundaries vertically until they reach L . Since we do not split the bottom side of R_t , we can recover R_t by extending only its right boundary. Since the length of segment $|ab|$ is integral, all the line segments of the resulting drawing have integral coordinates.

It is straightforward to remove an incomparable pair in $O(n)$ time, where n is the number of rectangles in \mathcal{R} . Since \mathcal{R} may contain at most $O(n)$ incomparable pairs, one can construct \mathcal{R}_c in $O(n^2)$ time. \square

Appendix B

Here we describe the details of processing a consumer R_p . Let p be the vertex that corresponds to R_p . Let d_p denote the degree of p , and let $\delta_t, \delta_b, \delta_l, \delta_r$ be the number of rectangles that are incident to the top, bottom, left and right sides of R_p , respectively. Let $\Psi_{tl}, \Psi_{tr}, \Psi_{bl}, \Psi_{br}$ be the number of contact points on the top-left, top-right, bottom-left, and bottom-right cords of R_p .

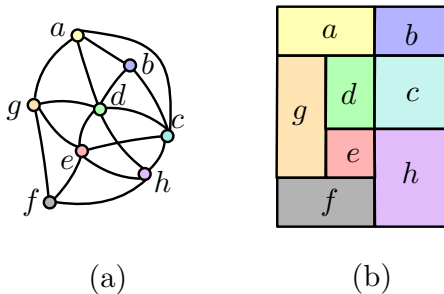


Figure 6: (a) A graph G . (b) A rectangle contact representation of G .

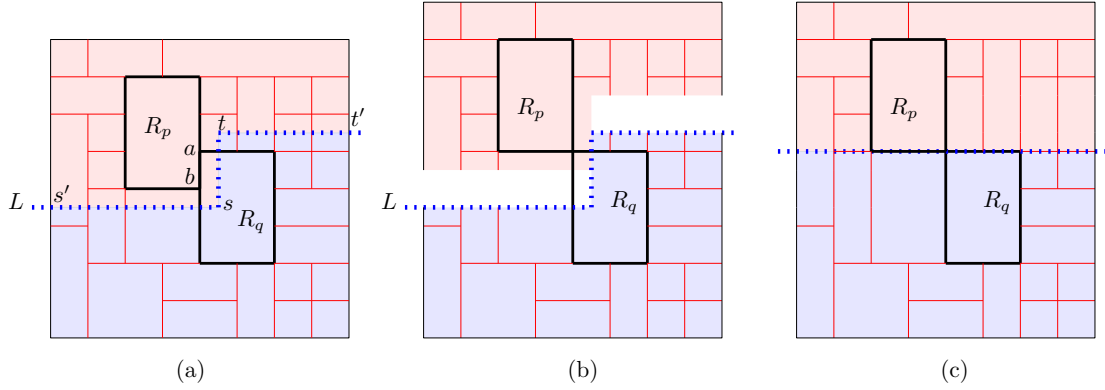


Figure 7: (a) A rectangle contact representation, which is not consistent, and a cut corresponding to ab . (b)–(c) Removal of segment ab .

We have numerous cases, depending on whether R_p is the consumer of one excess pair or of two. We must further distinguish by whether certain neighbours of R_p contain the x -range resp. y -range of R_p . (We will not always explicitly say in the text which neighbour is meant when speaking, e.g., of R_g ; this should be clear from the picture.) Finally we distinguish by the size and relationships between $\delta_t, \delta_b, \delta_l, \delta_r$. Unfortunately there appears to be no way to unify these cases into fewer. However, the following observation will often be used to argue correctness. Assume that we are in a setup where we can *saturate* one cord, i.e., add contacts such that (e.g.) $\psi_{tl} = \delta_P/2$. Then, as long as we assign all other contacts at P to other cords, all cords have at most $\delta_P/2$ contacts as required.

Case 1 (R_p is a consumer of exactly one excess pair). Without loss of generality assume that the excess pair $\{R_a, R_b\}$ is at the bottom-right corner of R_p , and R_b lies above R_a , e.g., see Fig. 5(a).

Case 1a ($R_p \subset_x R_a$). This case is illustrated in Fig. 5(a). Here we distinguish two scenarios depending on whether $\delta_l > d_p/2$ or $\delta_l \leq d_p/2$.

- Case ($\delta_l > d_p/2$): This implies that $\delta_r \leq d_p/2$.
 - If $R_b \subseteq_y R_p$, then we re-route the cords of R_p following Fig. 5(b) and saturate the bottom-left cord. We note that in Fig. 5, we have $R_{b'} \subset_x R_a$, which is merely an illustration. The modification works fine even when $R_a \subseteq_x R_{b'}$. The same applies to all the adjacencies that do not involve R_p .
 - If $R_p \subset_y R_b$ and $R_g \subseteq_x R_p$, then we follow Fig. 5(c) and saturate the bottom-left cord.

Observe that if R_g is a consumer, then the bottom-left corner of R_g will coincide with the top-left corner of R_p . This modification removes the excess pair from the bottom corners of R_p , but R_g still remains a consumer. The excess pair at the bottom corners of R_g will be removed when we process R_g .
 - If $R_p \subset_y R_b$ and $R_p \subset_x R_g$, then we follow Fig. 5(d) and saturate the top-left cord. Here the top-left cord of R_p cannot reach the top-left corner of R_p , which is fine since the adjacency between R_g and R_p is realized at the top-right corner of R_p , and since for each rectangle adjacent to the left of R_p , one of its two cords is extended to touch the cords of R_p . We will never need to choose between the top-left and bottom-left arms of R_p to process the remaining consumer rectangles.
- Case ($\delta_l \leq d_p/2$ and $R_{b'} \subseteq_y R_p$):
 - If $\delta_r > d_p/2$, then we follow Fig. 8(b) and saturate the bottom-right cord.

- If $\delta_r \leq d_p/2$ and $R_b \subseteq_y R_p$, then we follow Fig. 8(c)–(d) depending on whether $\delta_r \leq \delta_l$ or not.
 - If $\delta_r \leq \delta_l$ (Fig. 8(c)), then $\Psi_{tl} \leq \frac{\delta_t}{2} + O(1) \leq \Delta_p$, and $\Psi_{tr} \leq \frac{\delta_t}{2} + \delta_r + O(1) \leq \frac{\delta_t + 2\delta_r}{2} + O(1) \leq \frac{\delta_t + \delta_l + \delta_r}{2} + O(1) \leq \Delta_p$. If $\delta_r > \delta_l$ (Fig. 8(d)), then $\Psi_{tr} \leq \frac{\delta_t}{2} + \frac{\delta_r}{2} + O(1) \leq \Delta_p$, and $\Psi_{tl} \leq \frac{\delta_t}{2} + \delta_l + O(1) \leq \frac{\delta_t + 2\delta_l}{2} + O(1) \leq \frac{\delta_t + \delta_l + \delta_r}{2} + O(1) \leq \Delta_p$.
- If $\delta_r \leq d_p/2$ and $R_p \subseteq_y R_b$, then the modification is shown in Fig. 8(e). Note that $\delta_l \leq d_p/2$. Therefore, we can saturate Ψ_{tr} with $\min\{\delta_t, d_p/2\}$ contacts to have $\Psi_{tl} \leq \delta_l + \delta_t - \Psi_{tr} + O(1) \leq \Delta_p$.

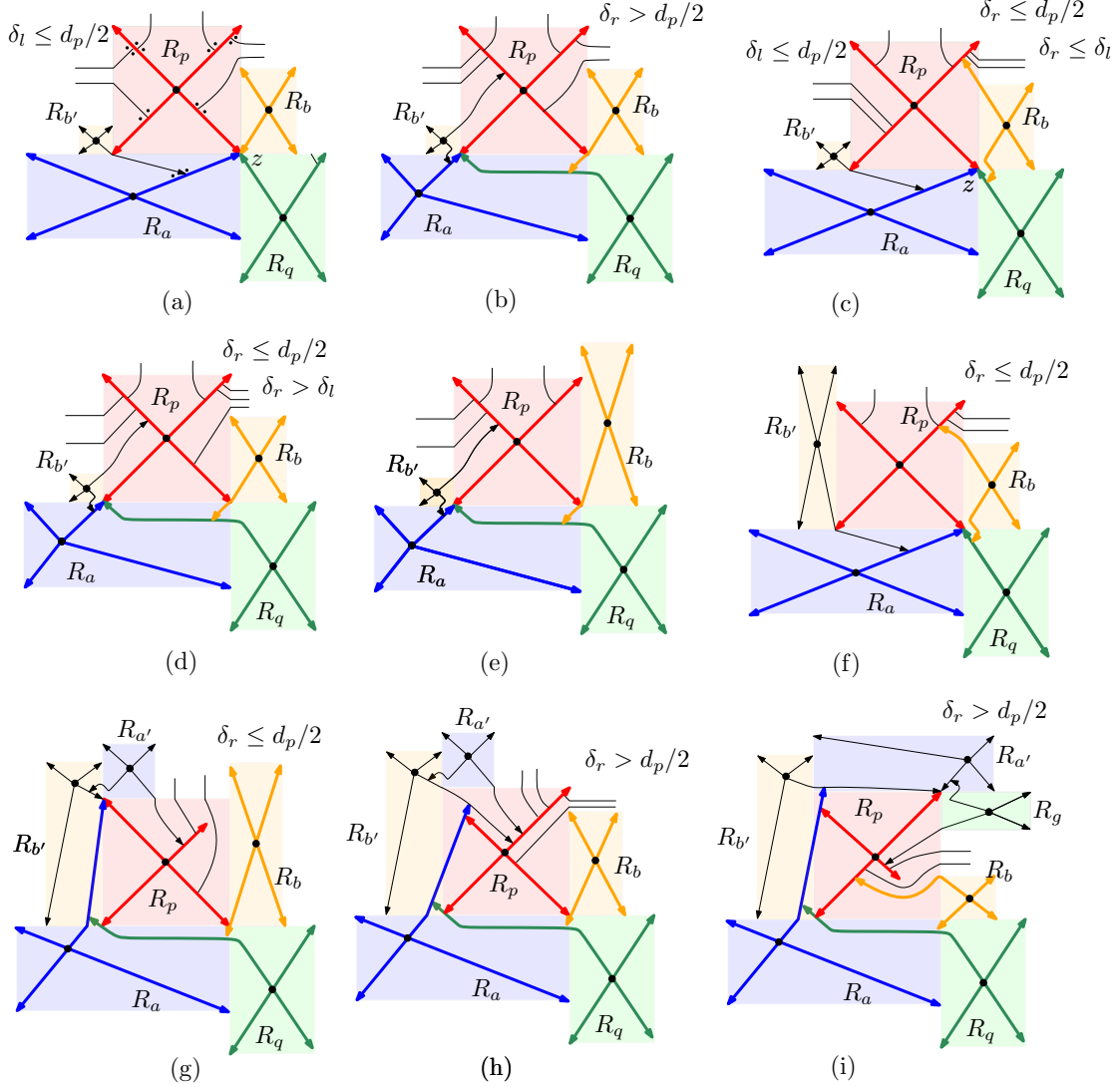


Figure 8: Illustration for Case 1a, where $\delta_l \leq d_p/2$. (a) Initial configuration. (b-i) Resolution.

- Case ($\delta_l \leq d_p/2$ and $R_p \subseteq_y R_{b'}$):
 - If $\delta_r \leq d_p/2$ and $R_b \subseteq_y R_p$, then we follow Fig. 8(f). We can saturate the top-right cord with $d_p/2$ incidences using edges from the top and the right.
 - If $\delta_r \leq d_p/2$ and $R_p \subseteq_y R_b$, then we follow Fig. 8(g). Here $\Psi_{tr}, \Psi_{br} \leq \delta_t/2 \leq \Delta_p$. Note that the top-right cord of R_p cannot reach the top-right corner of R_p , which is fine since the adjacency between R_b and R_p is realized at the bottom-right corner of R_p , and since for each rectangle adjacent to the top of R_p , one of its two cords

is extended to touch the cords of R_p . We will never need to choose between the top arms (similarly, bottom arms) of R_p to process the remaining consumer rectangles.

- If $\delta_r > d_p/2$ then we will always saturate the bottom-right cord. If $R_{a'} \subseteq_x R_p$, then we follow Fig. 8(h); and if $R_p \subseteq_x R_{a'}$, then we follow Fig. 8(i). We can distribute δ_r contacts such that $\Psi_{tr}, \Psi_{br}, \Psi_{tl} \leq \Delta_p$. In the latter case the bottom-right cord of R_p cannot reach the bottom-right corner of R_p , which is fine since the adjacency between R_b and R_p is realized at the bottom-left cord of R_p , and since for each rectangle adjacent to the right of R_p , one of its two cords is extended to touch the cords of R_p . We will never need to choose between the right arms of R_p to process the remaining consumer rectangles.

Case 1b ($R_a \subseteq_x R_p$). This case is illustrated in Fig. 9(a). Here we distinguish the scenarios whether $R_b \subseteq_y R_p$ or $R_p \subseteq_y R_b$.

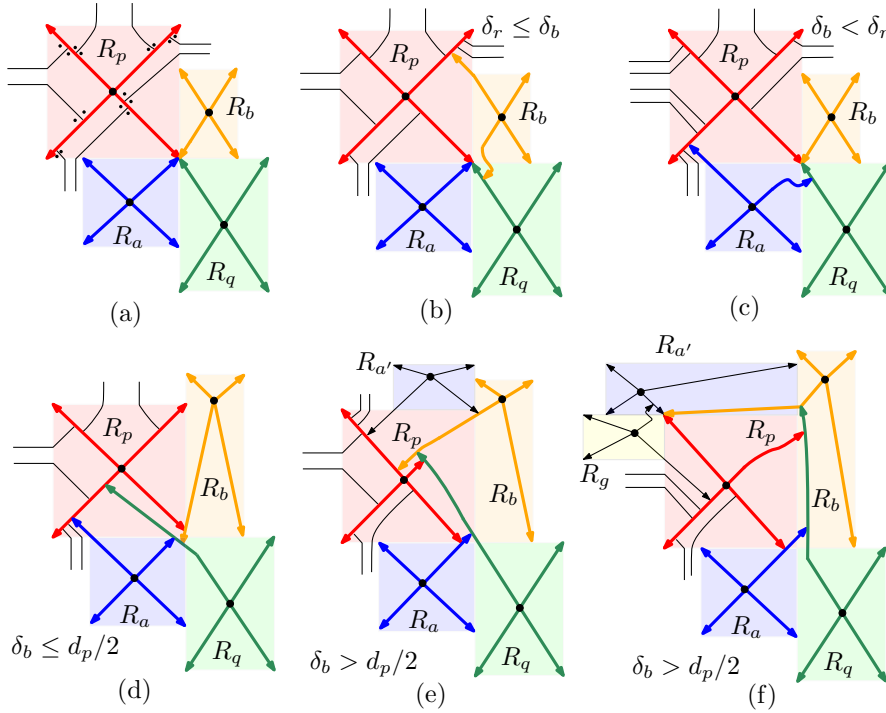


Figure 9: Illustration for Case 1b. (a) Initial configuration. (b-f) Resolution.

- Case ($R_b \subseteq_y R_p$):

If $\delta_r \leq \delta_b$, then we follow Fig. 9(b). It is straightforward to see that $\Psi_{bl}, \Psi_{tl} \leq \Delta_p$ and $\Psi_{br} \in O(1)$. Since $\delta_r \leq \delta_b$, $\Psi_{tr} \leq \frac{\delta_t}{2} + \delta_r \leq \frac{\delta_t + 2\delta_r}{2} \leq \frac{\delta_t + \delta_l + \delta_r}{2} \leq d_p/2$. If $\delta_b < \delta_r$, then we follow Fig. 9(c). The analysis for the contact points is symmetric.

- Case ($R_p \subseteq_y R_b$):

If $\delta_b \leq \delta_p/2$, then we follow Fig. 9(d) and can saturate the top-left cord since $\delta_\ell + \delta_t \geq \delta_p/2 - O(1)$. On the other hand, if $\delta_b > \delta_p/2$, then we distinguish between whether $R_{a'} \subseteq_x R_p$ or not. If $R_{a'} \subseteq_x R_p$, then we follow Fig. 9(e) and saturate the bottom-right cord. If $R_p \subseteq_x R_{a'}$, then we follow Fig. 9(d) and again saturate the bottom-right cord.

Case 2 (R_p is a consumer of two excess pairs). See Fig. 10(a). We consider three cases depending on whether any of $\delta_t, \delta_r, \delta_l$ or δ_b is larger than $d_p/2$ or not.

- Case ($\delta_t > d_p/2$):

In this case, we will always saturate the top-right cord. If $R_{b'}, R_b \subseteq_y R_p$, then we follow Fig. 10(b); if $R_p \subset_y R_b$ and $R_{b'} \subseteq_y R_p$, then we follow Fig. 10(c), and the case when $R_p \subset_y R_{b'}$ and $R_b \subseteq_y R_p$ is symmetric. Finally, if $R_p \subset_y R_b$ and $R_p \subset_y R_{b'}$, then we follow Fig. 10(d). Here the top cords of R_p cannot reach their corresponding corners, which is fine since the adjacencies $R_{b'}, R_p$ and R_b, R_p are realized at the top-right and bottom-right cords of R_p , and since for each rectangle adjacent to the top of R_p , one of its two cords is extended to touch the cords of R_p . Furthermore, we will never need to choose between the top arms of R_p to process the remaining consumer rectangles.

- Case ($\delta_b > d_p/2$):

In this case, we will always saturate the bottom-right cord. If $R_{b'}, R_b \subseteq_y R_p$, then we follow Fig. 10(e). If $R_p \subset_y R_b$ and $R_{b'} \subseteq_y R_p$, then we follow Fig. 10(f) or (g) depending on the placement of R_g . The case when $R_p \subset_y R_{b'}$ and $R_b \subseteq_y R_p$ is symmetric. Finally, if $R_p \subset_y R_b$ and $R_p \subset_y R_{b'}$, then we follow Fig. 10(h). Here the right cords of R_p cannot reach their corresponding corners, which is fine since the adjacencies R_q, R_p and R_b, R_p are realized at the top-right and top-left cords of R_p , and since for each rectangle adjacent to the bottom of R_p , one of its two cords is extended to touch the cords of R_p .

- Case ($\delta_l > d_p/2$):

In this case, we will always saturate the bottom-left cord. If $R_b \subseteq_y R_p$, then we follow Fig. 10(i). If $R_p \subset_y R_b$, then we follow Fig. 10(j) or (k) depending on the placement of R_g . In the latter case, the top-right and bottom-left cords of R_p cannot reach their corresponding corners, which is fine since the adjacencies $R_{q'}, R_p$ and R_b, R_p are realized at the bottom-right and top-left cords of R_p , and since for each rectangle adjacent to the left of R_p , one of its two cords is extended to touch the cords of R_p .

- Case ($\delta_r > d_p/2$):

This case is symmetric to the case when $\delta_l > d_p/2$.

- Case ($\delta_l, \delta_r, \delta_t, \delta_b \leq d_p/2$):

This case can be handled in the same way as the case when $\delta_t > d_p/2$, i.e., following the Fig. 10(b)–(d). We cannot always saturate a cord now, but by suitably splitting δ_t between two cords, we can ensure that all cords are balanced.

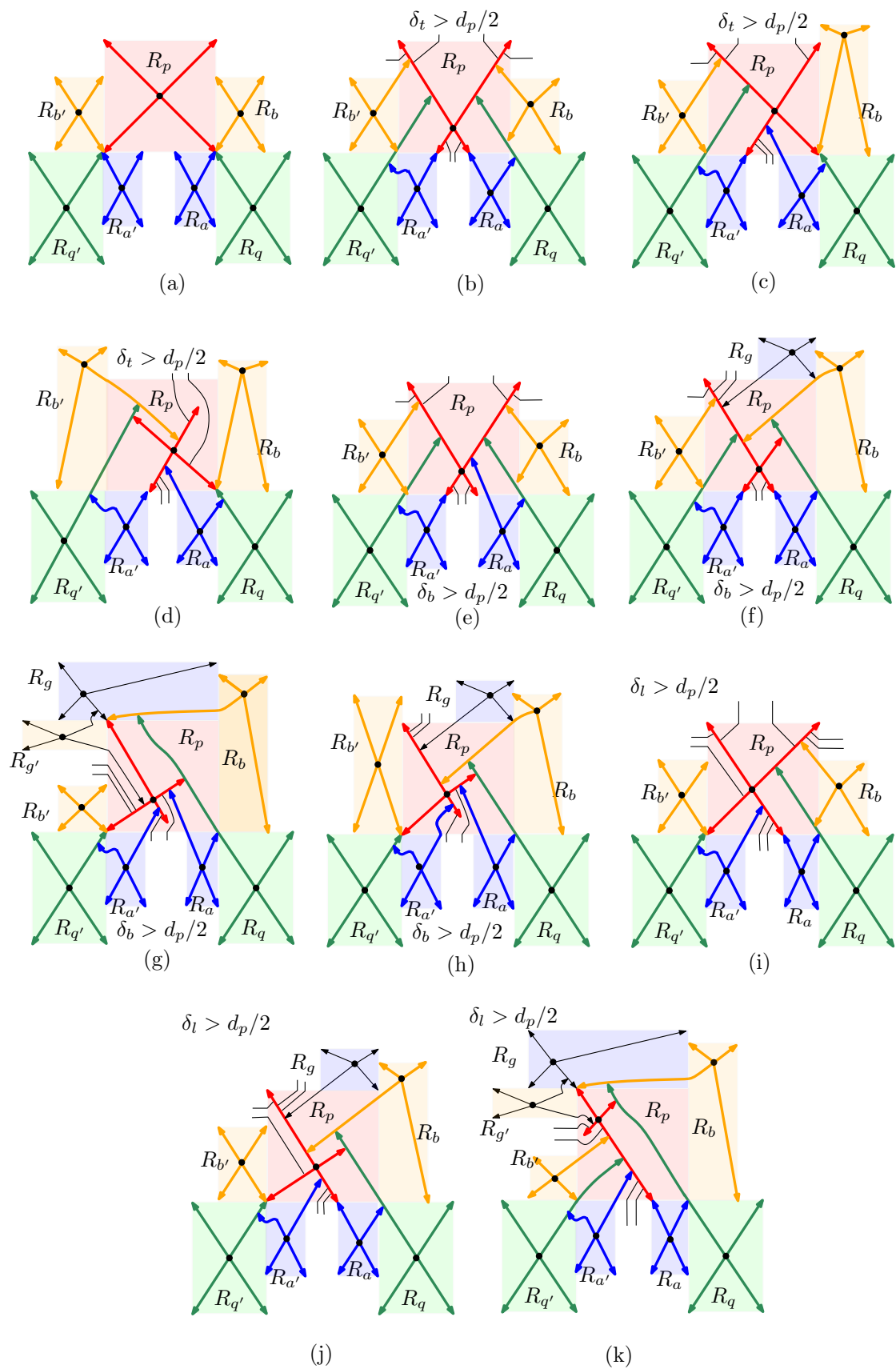


Figure 10: Illustration for Case 2. (a) Initial configuration. (b-k) Resolution.